Electronic transport and the localization length in the quantum Hall effect

M. Furlan

Swiss Federal Institute of Technology EPFL, CH-1015 Lausanne, Switzerland
and Swiss Federal Office of Metrology OFMET, CH-3084 Wabern, Switzerland

(Received 23 December 1997)

We report on recent experimental results from transport measurements with large Hall bars made of high-mobility GaAs/Al$_x$Ga$_{1-x}$As heterostructures. Thermally activated conductivities and hopping transport were investigated in the integer quantum Hall regime. The predominant transport processes in two dimensions are discussed. The implications of transport regime on prefactor universality and on the relation between ρ_{xx} and ρ_{xy} are studied. Particularly in the Landau-level tails, a strictly linear dependence $\delta\rho_{xy}(\rho_{xx})$ was found, with pronounced asymmetries with respect to the plateau center. At low temperatures, Ohmic (temperature-dependent) as well as non-Ohmic (current-dependent) transport were investigated and analyzed on the basis of variable-range hopping theory. The non-Ohmic regime could successfully be described by an effective electron temperature model. The results from either the Ohmic transport or from a comparison of Ohmic and non-Ohmic data allowed us to determine the localization length ξ in two different ways. The observed divergence of $\xi(\nu)$ with the filling factor ν approaching a Landau-level center, is in qualitative agreement with scaling theories of electron localization. The absolute values of ξ far from the ρ_{xx} peaks are compared with theoretical predictions. On one hand, discrepancies between the ξ results obtained from the two experimental methods are attributed to an inhomogeneous electric-field distribution. Extrapolation yields an effective width of dominant potential drop of about 100 μm. On the other hand, our analysis suggests a divergence of the dielectric function $\epsilon_r \propto \xi^\beta$ with $\beta \simeq 1$. [S0163-1829(98)05320-X]

I. INTRODUCTION

Transport measurements in the quantum Hall[1] regime have been widely used to investigate fundamental physics of electron conduction in the case of a quantized two-dimensional electron gas in strong perpendicular magnetic fields. If the energy separation between the Landau levels (LL's), i.e., the cyclotron energy $\hbar\omega_c$, is much larger than the LL linewidth, all electrons within the LL tails are considered to be localized. The localization length ξ characterizes the size of the space region in which the wave function of an electron, moving in an impurity potential, is not exponentially small. This characteristic length is believed to diverge with the Fermi level E_F approaching the LL center. In that limit, the divergence can be expressed according to a power law:

$$\xi(\nu) \propto |\nu - \nu_c|^{-\gamma}, \tag{1}$$

where $\nu = 2\pi l_B^2 n_e$ is the filling factor (with $l_B = \sqrt{\hbar/eB}$ the magnetic length and n_e the electron sheet density). The value ν_c corresponds to the position where E_F coincides with the LL center, and $\gamma \simeq 2.3$ is a critical exponent.[2–5] On the other hand, the localization length at the resistivity minima was recently predicted[6] to be on the order of the classical cyclotron radius (true for our samples, although depending on the phase diagram introduced in Ref. 6). The transport properties depend on disorder and on the temperature. Different dominant transport processes are distinguished for different temperature ranges. At intermediate temperatures (typically a few K), conductance is predominantly determined by electrons thermally activated to the nearest extended states. The

diagonal conductivity tensor component σ_{xx} then follows an Arrhenius law

$$\sigma_{xx}(T) = \sigma_{xx}^0 e^{-T_0/T}. \tag{2}$$

The activation energy $k_B T_0$ corresponds to the distance between the Fermi energy E_F and the percolation level E_c. In several works,[7–10] the universality and possible dependences of the prefactor values σ_{xx}^0 were studied.

Based on considerations of localization and percolation (and in the limit $\sigma_{xx} \ll e^2/h$), a similar thermally activated behavior is expected for the deviation

$$\delta\sigma_{xy}(T) = \sigma_{xy}(T) - \frac{e^2\nu_0}{h}$$

from the quantized Hall conductivity, where ν_0 is the integer filling factor at the plateau center. In spite of the importance of understanding the reasons and processes leading to a possible deviation from the quantized values, a clear and unambiguous distinction between pure thermal activation and other effects (e.g., sample-dependent mixing of the tensor components) has not yet been experimentally achieved. At integer filling factors and sufficiently wide cyclotron gaps, however, a linear dependence $\delta\sigma_{xy}(T) \propto \sigma_{xx}(T)$ has often been observed.[11] Unfortunately, such experiments have not been extended to the Hall plateau regions further away from the plateau centers. In the dissipative regime of plateau transitions, where the Shubnikov–de Haas (SdH) peaks emerge, the situation is again different: σ_{xy} and σ_{xx} are not independent variables, but are described by a two-parameter renormalization-group theory,[3,12] satisfying the so-called semicircle rule.[13]

Whereas many experiments were concerned with measurements at the σ_{xx} minima only, others[2,5,12,14] especially concentrated on the transition regions. In spite of large theoretical efforts, experiments to link the different regimes in order to complete the picture of thermally activated transport in the quantum Hall effect are still missing.

With decreasing temperature, the longitudinal conductivity becomes exponentially small, and an electron conduction mechanism known as variable-range hopping (VRH) becomes the dominant transport process.[15] Several attempts to describe the measured $\sigma_{xx}(T)$ behavior in the hopping regime with

$$\sigma_{xx} \propto e^{-(T_1/T)^\alpha} \qquad (3)$$

were reported.[16,17] While Eq. (3) describes the Mott hopping[18] with $\alpha = \frac{1}{3}$ ($\frac{1}{4}$) in two (three) dimensions in the absence of a Coulomb gap, a suppression of the density of states near the Fermi level due to Coulomb interactions[19] leads to a soft Coulomb gap,[20] and expression (3) with an exponent $\alpha = \frac{1}{2}$ was derived:

$$\sigma_{xx}(T) = \sigma_{xx}^T e^{-\sqrt{T_1/T}}, \qquad (4)$$

where

$$k_B T_1(\nu) = C \frac{e^2}{4 \pi \epsilon_r \epsilon_0 \xi(\nu)}, \qquad (5)$$

with the numerical constant $C \approx 6.2$ in two dimensions,[21] the dielectric function $\epsilon_r \approx 13$ (value for GaAs), and the vacuum permittivity ϵ_0. The hopping behavior (4) was also derived in Refs. 22–24, although with different coefficients for T_1 and σ_{xx}^T. The role of the prefactor σ_{xx}^T, i.e., whether it is temperature dependent or not, was widely disputed and still remains an unsolved problem. Experimentally, a prefactor proportionality $\sigma_{xx}^T \propto 1/T$ was usually observed.[16,17,25,26]

Although the quantum Hall effect can successfully be described by means of the linear-response theory at low current levels, the non-Ohmic transport observed at high electric fields is not yet well understood. Different models were proposed to explain the behavior in the current region below the critical breakdown current: inter- and intra-LL transitions due to high local electric field[27] (tunneling or emission of phonons), increase in the number of delocalized states in the LL,[28] or the production of superheated electrons.[29] Experimentally, an essentially exponential dependence of the longitudinal resistivity on current has most often been observed. In a recent model,[30] the non-Ohmic transport in the quantum Hall regime was discussed on the basis of the theory of hopping in a strong electric field.[31] At low temperatures, non-Ohmic transport in the VRH regime is then expected to show a behavior like

$$\sigma_{xx}(J) = \sigma_{xx}^J e^{-\sqrt{\mathcal{E}_1/\mathcal{E}_H}}, \qquad (6)$$

where $\mathcal{E}_H$ is the Hall electric field across the sample, and

$$\mathcal{E}_1 = \frac{2 k_B T_1}{e \xi} \qquad (7)$$

is a characteristic value related to the hopping temperature. This electric-field-dependent hopping transport model is based on the idea of the existence of a quasi-Fermi level tilted by the electric field. As a consequence, the local Fermi distribution is formed corresponding to an effective temperature $T_{\text{eff}} \propto \mathcal{E}_H \xi$. Hence, in analogy to the Ohmic hopping transport (4) in the quantum Hall regime, the non-Ohmic conductivity in the limit of vanishing temperature is then immediately given by Eq. (6) for increasing electric field.

Both the temperature and current-dependent VRH conductivities in Eqs. (4) and (6) explicitly depend on the localization length ξ via the characteristic values T_1 and $\mathcal{E}_1$ [Eqs. (5) and (7)]. To test the predictions, it is interesting to compare experimental results (namely, the extracted ξ) on the basis of the discussed hopping theory. While Eq. (5) also contains a dependence on ϵ_r, the localization length in Eq. (7) is a pure function of characteristic values obtained from experiment: a comparison of the measured conductivities $\sigma_{xx}(T)$ and $\sigma_{xx}(J)$ relates the current J to an effective temperature like

$$k_B T_{\text{eff}}(J) = e \xi \frac{\rho_{xy} J}{2 L_y}, \qquad (8)$$

where L_y is the sample width. The localization length ξ can therefore be determined without explicitly knowing the exact behavior of the prefactors.

In the present paper, we report on experimental results from extensive transport measurements, covering the ranges of thermally activated and VRH transport in the integer quantum Hall effect. The subsequent text is organized as follows: the experimental conditions and the sample properties are presented in Sec. II. The experimental results in Sec. III are divided into three parts. First, the important results from thermally activated transport measurements are summarized, and the relations between the resistivity tensor components are discussed. The other two parts are devoted to either temperature or current-dependent measurements in the VRH regime. Section IV gives a discussion about the determination of $\xi(\nu)$. Possible reasons for discrepancies between results, obtained from different experiments, are considered. Conclusions are given in Sec. V.

II. SAMPLE PROPERTIES AND MEASUREMENT TECHNIQUE

For the transport experiments, we have used Hall bars made of GaAs/Al$_x$Ga$_{1-x}$As heterostructures. These are considered as ''good'' samples from the metrological point of view: they have wide Hall voltage plateaus ($\Delta B \approx 2$ T for plateau two), high critical breakdown currents ($J_c > 10^{-4}$ A), and low contact resistances (typically well below 1 Ω). Nonideal contacts, i.e., with high resistance, introduce a nonequilibrium edge-bulk electron distribution. At short distances and in the linear low-current regime, such a nonequilibrium situation leads to the observation of the reported nonlocal resistances.[32,33] In this context, it is well established that high contact quality is crucial for the observability of the exact quantization,[34,35] as well as for correct determination of the longitudinal resistivity in Hall bars. Our samples are also rather large (bar width and contact distances typically 1 mm) in order to omit narrow channel effects or poor equilibration between the probes. We are stressing these facts to empha-

TABLE I. Electron sheet density n_e, mobility μ_e, and spacer thickness d for the two Hall bar GaAs/Al$_x$Ga$_{1-x}$As heterostructures. The corresponding Fermi wave vector k_F and the elastic mean free path l_{mfp} are calculated. $L_{x,\mathrm{min}}$ is the distance between two consecutive voltage probes, and L_y is the Hall bar width. Sample A was produced at the Niels Bohr Institute (København, Denmark), sample B at EPFL (Lausanne, Switzerland).

Sample	n_e (m^{-2})	μ_e (T^{-1})	d (nm)	k_F (m^{-1})	l_{mfp} (μm)	$L_{x,\mathrm{min}}$ (mm)	L_y (mm)
A: HCØ 130/92	3.09×10^{15}	132	25	1.39×10^8	12.1	1.50	0.50
B: EPF 277/5	4.74×10^{15}	38.8	10	1.73×10^8	4.4	1.25	1.00

size that our samples did not suffer nonlocal transport, in the sense as described in Ref. 36.

For the present investigations, we concentrate on two samples from different production sources and with different properties, as listed in Table I. Further details on the samples may also be found in Ref. 34. Each Hall bar had three equidistant voltage probes on each side, which, upon injection of a dc current J, were all measured simultaneously, yielding the potential drop V_{ij} across any contact pair combination. The resistances $R_{ij} = V_{ij}/J$ were determined from the mean value from the measurements with both current polarities. Thus, with the dc technique, thermoelectric effects or any instrumental offsets were safely canceled, while the information was still available to account for current path dependent effects: at very low current levels (typically below 10^{-8} A in our samples), nonlinear and in some cases strongly asymmetrical behavior can be observed.[37] This low-current regime was excluded from our data analysis, and we will only discuss transport either at current levels where linear response is applicable or in the non-Ohmic regime at higher currents.

The experiments were performed by varying current J, temperature T, and magnetic field density B. We want to restrict the present discussion to the range of high-magnetic-field densities corresponding to filling factors within $1.5 < \nu < 4.5$, and particularly concentrate on the plateau regions. According to this range, the plateaus around the filling factors $\nu \approx 2$, 3, and 4 are called plateaus 2, 3, and 4, respectively. The spin-split LL with the index $N=1$, leading to the third plateau, was well resolved at low temperatures, i.e., negligible overlap of the energy bands. Two types of experiments were performed extensively: (a) at fixed ν the current was set to $|J| = 1$ μA, and the temperature varied in the range 300 mK $\leq T \leq 20$ K; or (b) the temperature was kept constant at $T = 324 \pm 12$ mK, and the current varied in the range 1 μA $\leq |J| \leq 100$ μA. The temperature measurement was performed with a Speer resistor and a capacitance thermometer, both calibrated on the basis of a germanium thermometer at $B=0$, and then extended with the necessary corrections due to magnetoresistive effects. The accuracy of our thorough temperature measurement was comparable to the uncertainties given for the calibration curve (from Lakeshore) of the germanium sensor. In experiment (a), the temperature was swept very slowly (typically several hours for a change in temperature by one order of magnitude) in order to guarantee thermal equilibration as well as sufficient statistics in the experimental data. No hysteresis or other variations between consecutive T sweeps could be observed. In case (b), special care has been taken during the experiments as well as in the offline data analysis to keep the dissipation at

a negligible level, i.e., no significant temperature variation of the ^{3}He bath.

The sample contact resistances were periodically controlled during the experiments in order to monitor any deviations of the sample quality that could lead to systematic errors. Upon proper and careful sample handling, the experiments could be continuously carried out during several days with perfect reproducibility and with no significant change in sample properties. This was an essential condition to allow a comparison of the data from different runs, since thermal cycling generally also changes sample characteristics, like the mean electron sheet density and the local charge and potential distribution.

From the measured longitudinal and transverse resistances R_L and R_H, respectively, and with the usual assumption of a homogeneous sample, we determined the resistivity tensor components $\rho_{xx} = \rho_{yy} = R_L L_y / L_x$ and $\rho_{xy} = -\rho_{yx} = R_H$, with the distance L_x between the voltage probes and the width L_y of the Hall bar. The conductivity tensor is given by $\sigma_{\mu\nu} = (\rho^{-1})_{\mu\nu}$. We present results for both quantities, depending on the theories referred to and the appropriate range of values considered.

III. EXPERIMENTAL RESULTS

In order to make sure that the temperature-dependent experiments were not influenced by electron heating effects, we performed measurements of SdH oscillations at our lowest ^{3}He bath temperature (300 mK) and varied the bias current. Figure 1 shows such SdH traces $\rho_{xx}(B)$ for sample A with current levels 30 nA $\leq J \leq 30$ μA, together with the corresponding Hall resistivities $\rho_{xy}(B)$. A clear decrease of the SdH peaks is observed with decreasing J. While the oscillations strongly depend on J at high current levels, they saturate at about $J \lesssim 1$ μA. Therefore, we have chosen $J = 1$ μA as a compromise between negligible electron heating and maximum sensitivity to low resistivities.

Also apparent in Fig. 1 is the typical strong asymmetry between the SdH peaks corresponding to the up and down spin-split LL's.[38,39] This effect is qualitatively well explained by the theory[39,40] of different equilibration probabilities of the edge and bulk channels at the sample edges due to different distances in the confining potential. An increased $\mathcal{E}_H$ tilts the potential, and therefore reduces the channel distances. However, it turned out that one has to be cautious with a straightforward application of the theoretical formulation[39,40] to the experimental data: depending on how the results are analyzed (data range and choice of free fit parameters) we alternatively obtain equilibration lengths, which are by orders of magnitude larger than our sample
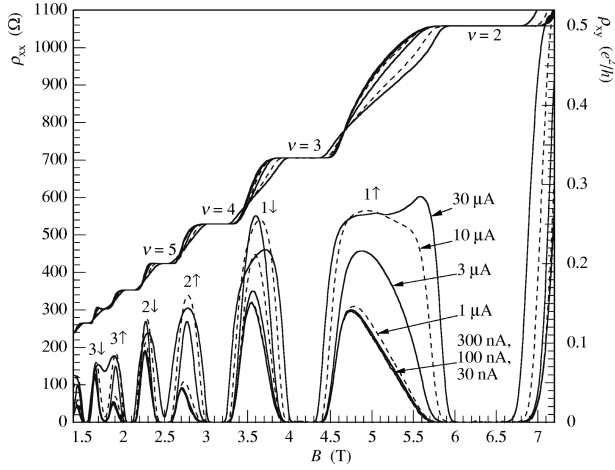
FIG. 1. SdH oscillations $\rho_{xx}(B)$ and Hall resistivities $\rho_{xy}(B)$ at $T \simeq 0.3$ K for different bias currents (sample A). The ρ_{xx} peaks are labeled with their corresponding LL index and the spin polarization, the ρ_{xy} plateaus with the filling factor ν_0.

size. Furthermore, we see no difference in the resistivities measured at different contacts and at different distances. The problem of extracting, in some cases, a physically meaningful equilibration length has already been realized in Ref. 33. The discrepancy may be attributed to the requirement of a homogeneous carrier density in the model, which is not necessarily fulfilled particularly in our high-mobility samples.

Another argument for the observed asymmetries of SdH peaks was given in Ref. 38, according to which the density of states (DOS) becomes asymmetric due to an unequal contribution of attractive and repulsive scatterers. From our data analysis (cf. the note in Sec. III B), we could not find any significantly asymmetric DOS in our samples. Hence we have to reject in our case the picture of DOS-correlated asymmetries of the measured SdH peaks.

A. Thermal activation

We have recently reported on experimental results of thermally activated longitudinal conductivities for our high mobility samples in the quantized plateau regimes.[41] Clear activated behavior, according to Eq. (2), was observed in an intermediate-temperature range $T \approx 1, \ldots, 10$ K, and typically over at least two decades in σ_{xx}. Measurements with lower bias currents by one order of magnitude led to the same results of the activated data, justifying the neglect of electron heating due to sufficiently low current density. The activation energies $k_B T_0$ were extracted from fitting Eq. (2) to the maximum slopes of the data points. At $\nu_0 = 2$ and 4, they were found to be equal to half of the LL spacing $\hbar \omega_c / 2$ within experimental uncertainties. This is in perfect agreement with expectations, and with the fact of negligible spin energy $g_0 \mu_B B \ll \hbar \omega_c$. At $\nu_0 = 3$, increased activation energies compared to the bare spin-splitting energy were observed due to an effectively enhanced g factor g^* $\approx 3.5, \ldots, 5.4$ as a result of exchange interaction[42] (larger g^* was found for higher-mobility samples). This is consistent with former experiments, where a g-factor enhancement at odd ν_0 by about one order of magnitude (compared to the GaAs bare value $g_0 = 0.44$) was reported.[43] Very recently,
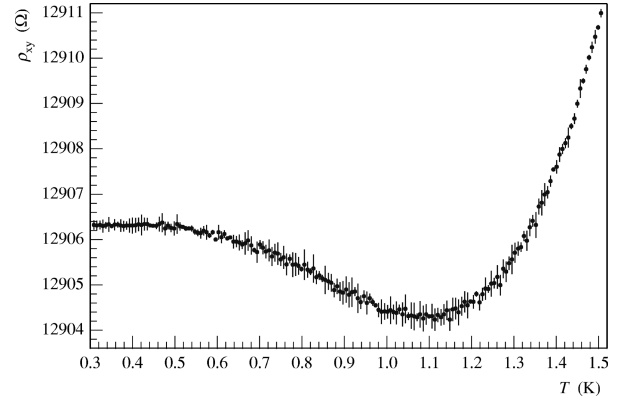

FIG. 2. Temperature-dependent transverse resistivity $\rho_{xy}(T)$ on the high-B plateau side. The dip around $T \approx 1$ K is due to a geometrical mixing of V_x into V_H.

however, one group[44] found an enhanced Landé factor g^* ≈ 5.2, but with a spin gap proportional to B. This cannot be explained by the model of exchange enhancement.

Furthermore, in agreement with a recent prediction[9] for high-mobility samples with a long-range impurity potential, the prefactors σ_{xx}^0 in Eq. (2) closely approached the universal value $2e^2/h$ at ν_0: the mean value of all σ_{xx}^0 ($\nu_0 = 2$, 3, and 4) and from all investigated samples was $(2.02 \pm 0.11)e^2/h$. However, at $|\nu - \nu_0| \gtrsim 0.05$ around even ν_0, the prefactors unexpectedly dropped by about one order of magnitude. While another group reported similar behavior[45] and attributed it to a contribution of VRH conduction, we have doubts about this interpretation for such elevated temperatures up to 10 K. We always observed one single exponential slope at intermediate temperatures and, what we consider the hopping contribution, a clear upward curvature from the Arrhenius Law at $T \lesssim 1$ K (cf. Fig. 1 in Ref. 41, and the discussion in Sec. III B of this paper). Our data at 1 K $< T < 10$ K and away from ν_0 are rather consistent with the picture of conduction via extended states in the case of a short-range impurity potential,[8] although we currently do not understand the reason for the abrupt regime crossover. A possible reason for the reduced prefactors is also an effective temperature dependence in the activation energy due to the adjustment of E_F, in order to keep the number of particles constant. As the Fermi level moves away from the nearest LL with increasing temperature, the observed prefactors become smaller than in the case of a temperature-independent E_F. This effect obviously does not occur in the special case of electron-hole symmetry with E_F in the middle between two LL's (minimum of the DOS), yielding the observed universal σ_{xx}^0 values. Irrespective of the reasons for the prefactor behavior, the narrow range around ν_0, where we have found $\sigma_{xx}^0 \simeq 2e^2/h$, can, however, explain the scattering of prefactor values experimentally observed by other groups.[46]

The investigation of the thermally activated behavior of the transverse resistivity $\rho_{xy}(T)$ (or conductivity) is complicated by a mixing of longitudinal voltage V_x into the Hall voltage V_H. Figure 2 shows a measurement of $\rho_{xy}(T)$ on the high-B plateau side ($\nu \approx 1.8$). The observed decrease of $\rho_{xy}(T)$ is independent of current polarity, magnetic-field direction, and contacts (for the same sample). It is explained by
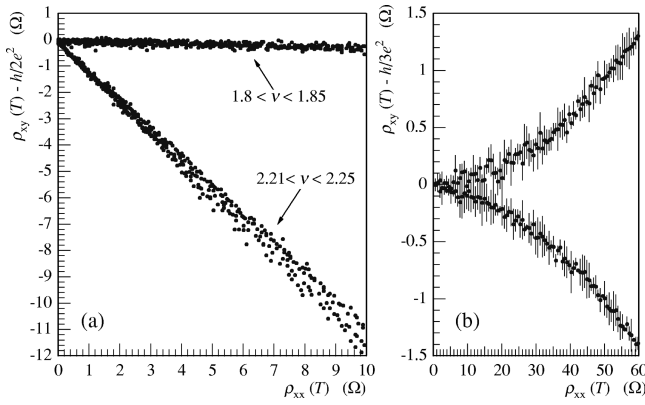
FIG. 3. Left (a): temperature-driven flow lines of $\delta\rho_{xy}(T)$ vs $\rho_{xx}(T)$ at the low-B ($\nu \approx 2.23$) and high-B ($\nu \approx 1.82$) plateau sides for low ρ_{xx} values (sample B). Right (b): temperature-driven resistivities as in (a), but for smaller $|E_F - E_c|$ (on the third plateau at $\nu = 3.06$ and 2.94). In this case $\rho_{xy}(T)$ is corrected to account for the geometrical mixing effect, according to Eq. (9).

a geometrical mixing[47] of V_x over the finite probe arm width w_p into V_H, yielding an effectively measured

$$\rho_{xy}^{\text{meas}}(T) = \rho_{xy}(T) - \frac{w_p}{L_y}\rho_{xx}(T). \qquad (9)$$

The geometrical ratio is $w_p/L_y = 3\%, \ldots, 14\%$ for our different samples, and Eq. (9) satisfactorily accounts for the observed mixing effect within experimental uncertainties. However, a more general and quantitatively more accurate measure of the $\rho_{xy}(T)$ behavior can be acquired by plotting $\rho_{xy}(T) = h/e^2\nu_0 + \delta\rho_{xy}(T)$ versus $\rho_{xx}(T)$. When the Fermi energy E_F is far enough from the percolation level E_c, and T is not too high (but still above the VRH regime), i.e., low ρ_{xx} values, we observe a strictly linear behavior of the temperature-driven $\delta\rho_{xy}/\rho_{xx}(\sim -\delta\sigma_{xy}/\sigma_{xx})$ typically over three decades in ρ_{xx}, as shown in Fig. 3(a). While more complicated temperature dependences of the prefactors in the thermal activation formulas were predicted,[10] our results show that the temperature-driven dependence $\delta\rho_{xy}(\rho_{xx})$ is dominated by the exponential term $\exp(-T_0/T)$ in the considered regime. For the case of higher temperatures and/or decreasing T_0, a crossover to a quadratic dependence $\delta\rho_{xy} \propto \rho_{xx}^2$ was observed, in agreement with finite-size scaling theories[48] and the so-called semicircle rule.[13] A measurement of activated behavior in this regime, taken on the third plateau, is shown in Fig. 3(b). In this case, E_F is in the spin gap and T_0 is consequently lower. Also, ρ_{xy} is corrected according to Eq. (9) to account for the mixing effect.

Now we want to draw more attention to the former case of linearly related $\delta\rho_{xy}(\rho_{xx})$. The slopes of the temperature-driven $\delta\rho_{xy}(\rho_{xx})$, obtained from linear fits to the measured data points, are shown in Fig. 4 as a function of ν (full points). The results on the even numbered plateaus show a strong asymmetry with respect to the plateau center [cf. also Fig. 3(a)]. This observation was reproduced with all our investigated high-mobility GaAs/Al$_x$Ga$_{1-x}$As heterostructures, and was independent of current polarity, magnetic-field direction, or contact pairs. The values on the high-B plateau side (low ν) are close to the correction $-(w_p/L_y)$ for geometrical mixing (9) within experimental uncertainties, as dis-
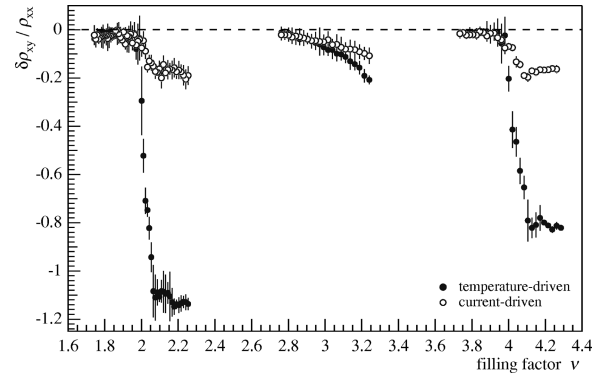

FIG. 4. Fit results for the slopes from the linearly related $\delta\rho_{xy}/\rho_{xx}$ (sample B). The full points ● are the temperature-driven data from experiment (a), the open circles ○ are from the current-dependent experiment (b).

cussed above. This result implies that in this plateau range $\rho_{xx}(T)$ is strongly enhanced relative to $\delta\rho_{xy}(T)$. On the low-B plateau side (high ν), however, this is not the case: slopes of order unity were found. We attribute this asymmetrical behavior to different longitudinal transport regimes, depending on the position of the Fermi energy E_F. This leads to a picture of either dominantly percolating empty or percolating full transport.[49] In the percolating empty regime (E_F in the low-energy LL tail), scattering occurs only between edge channels. In contrast, the interplay between edge and bulk states in the percolating full regime (E_F in the high-energy LL tail) leads to an increased backscattering probability with enhanced resistivities measured. Observation of a similar asymmetrical behavior and a model of distinct transport regimes have recently been reported.[50] The interpretation of different longitudinal transport regimes is also consistent with the experimentally evident asymmetries of the thermal activation prefactors[41] on even-numbered plateaus, where

$$\frac{\sigma_{xx}^0(\nu_0 - \delta\nu)}{\sigma_{xx}^0(\nu_0 + \delta\nu)} \approx 6$$

was observed [see Fig. 3(b) in Ref. 41]. This may also account for the peculiar discontinuity of the prefactor σ_{xx}^0 at $\nu = 3$, as we observed in some of our samples. We want to stress again that the transport phenomena discussed here are not to be confused with experimental observations of the anomalous QHE with nonideal contacts, which selectively probe only some poorly equilibrated edge channels. Our data neither depend on the longitudinal probe distance, nor are the results compatible with a temperature-dependent equilibration length.[51] The extrapolated Hall resistivities $\rho_{xy}(\rho_{xx} \to 0)$ perfectly coincide with the quantized values $h/e^2\nu_0$.

A basic result of the observed proportionality $\delta\rho_{xy}(T) \propto \rho_{xx}(T)$ is, besides the geometrical mixing effect (9), the indirect determination of the activation energy in $\delta\rho_{xy}(T)$: both resistivity tensor components essentially follow the same exponential behavior, which implies the same activation energy $k_B T_0$. Although this is not a spectacular result but rather an experimental confirmation of general theoretical consensus, not much significant and conclusive data about the activation energy in $\delta\rho_{xy}(T)$ have yet been published. The difference between $\delta\rho_{xy}$ and ρ_{xx} for E_F far from
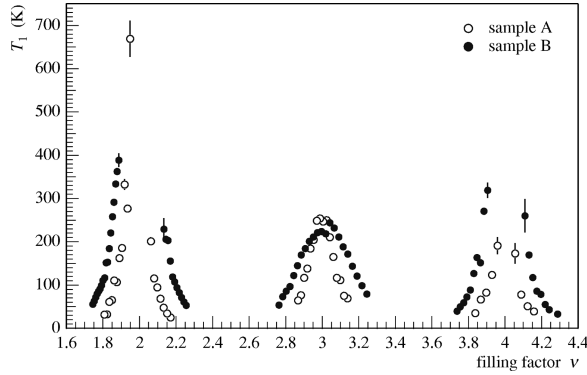
FIG. 5. Characteristic hopping temperature T_1, according to Eqs. (4) and (5), and extracted from the experimental data in the VRH regime at $T \lesssim 1$ K. The best fit to the data was found with a prefactor proportional to $1/T$. Around even ν_0, no data points are available due to unmeasurably small resistivities ρ_{xx} at low T.

E_c is concluded to be a consequence of different prefactors only. The prefactors themselves depend on ν (Fig. 4).

At this point we should emphasize again that the temperature-driven resistivities shown in Fig. 3 and the results in Fig. 4 correspond to the temperature range $T \gtrsim 1$ K, where transport is dominated by conduction via electrons, which are thermally activated to extended states. At lower temperatures, where VRH becomes important, the temperature-driven slopes $\delta\rho_{xy}/\rho_{xx}$ were found to be equal to the ratio $-(w_p/L_y)$ for almost our entire plateau range, i.e., only due to the geometrical mixing effect. This is consistent with the theoretical prediction[23] of a negligibly small VRH contribution to $\delta\rho_{xy}$ compared to ρ_{xx}.

Results from current-driven resistivities obtained in experiment (b), i.e., in the non-Ohmic regime, are also shown in Fig. 4, and will be discussed in Sec. III C.

B. Variable-range hopping

As mentioned in Sec. III A, the temperature-dependent longitudinal conductivities were observed to deviate from the simple exponential Arrhenius behavior (2) at low temperatures $T \lesssim 1$ K. In this range, where a contribution of VRH conduction according to Eq. (3) is considered, the best fit to our experimental data was obtained with $\alpha = \frac{1}{2}$ and a temperature-dependent prefactor $\sigma_{xx}^T \propto 1/T$, in agreement with other experiments.[16,17,25] The extracted characteristic hopping temperature T_1 is shown in Fig. 5 as a function of ν. However, due to our rather limited low-T range, our fitting procedure is not very sensitive to the prefactor behavior, and we cannot conclusively rule out other temperature dependences of the prefactors. In the case of fitting with a temperature-independent σ_{xx}^T (and accepting a slightly worse agreement between the fit function and the data points), we obtain values for T_1 which are typically 20% larger than those shown in Fig. 5. Our T_1 results can therefore be considered to have a maximum uncertainty of this magnitude.

According to the theory of Ref. 22, the preexponential factor $\sigma_{xx}^T = e^2 \gamma_0/k_B T$ contains the material parameter γ_0, which is essentially a material constant, depending on the electron-phonon coupling strength. We observed, however, a pronounced asymmetry of γ_0 with respect to the plateau cen-

ters (not shown here), similar to the reported prefactor asymmetries of thermally activated σ_{xx} at higher T. On the low-ν plateau side, the values were about one order of magnitude larger than on the high-ν side. This result can certainly not be understood in terms of electron-phonon scattering only. We have estimated the DOS of the two-dimensional electron gas either by means of the activation energies $k_B T_0(\nu)$ and with the procedure proposed in Ref. 52, or from the characteristic temperatures T_1 according to the hopping model in Ref. 22. As mentioned above, the unequal contribution of attractive and repulsive scatterers in high-mobility heterostructures may be taken to be responsible for the asymmetries of the DOS,[38] having an influence, e.g., on the shape of SdH peaks. Within our ν range, the DOS does not show any significant asymmetries that could account for the dramatic prefactor behavior. We interpret the systematic asymmetries of the prefactors again with different transport regimes, depending on the position of E_F in the LL tail relative to the mobility edge (as discussed in Sec. III A).

With respect to our studies, there has been only one published experiment[16] up to now with a thorough quantitative investigation and useful data on hopping transport at the resistivity minima. From their analysis based on the hopping theory of Ref. 22, the authors claimed to extract values for T_1, which are more than one order of magnitude too small (implying a much too large DOS compared to the zero field value). In contrast to their results, our T_1 values far in the LL tails are well consistent with the mentioned hopping theory.[22] However, at the resistivity minima, the predictions for T_1 in Ref. 22 virtually coincide with those in Refs. 15 and 20 [i.e., Eq. (5)] for our samples at low ν. Hence, from the results around the plateau centers, we are not able to give precedence to either of the two models. On the other hand, however, the theory with the assumption[22] of Gaussian localization of the electron wave function $\psi(r) \propto e^{-r^2/4l_B^2}$ has been criticized,[30] with the argument that the tails of the wave function have a simple exponential form[53] $\psi(r) \propto e^{-|r|/\xi}$. Furthermore, it was mentioned above that the observed prefactor asymmetries are not consistent with the theoretical prediction in Ref. 22. Therefore, we will base our further analysis on the VRH theory as developed in Refs. 15, 20, and 30, together with Eq. (5).

C. Non-Ohmic transport and effective electron temperature

Several studies on the current dependent non-Ohmic transport were previously published, as mentioned in Sec. I. Before examining the applicability of the models to our experimental results, we shall first consider the current-driven relation between the measured $\rho_{xy}(J)$ and $\rho_{xx}(J)$, obtained from experiment (b). Similarly to the temperature-driven resistivities (Sec. III A), we found an essentially linear behavior of the current-driven $\rho_{xy}(\rho_{xx})$ typically over three decades of ρ_{xx}. The results for the slopes are shown in Fig. 4 (open circles). The same asymmetries were observed as in the case of experiment (a), but with significantly smaller values. On the low-ν plateau side, the slope values from both experiments coincide, i.e., they correspond to the geometrical mixing coefficient $-(w_p/L_y)$, according to Eq. (9). Thus we can conclude nothing about a possible difference in the actual behavior and the relations between the resistivities in
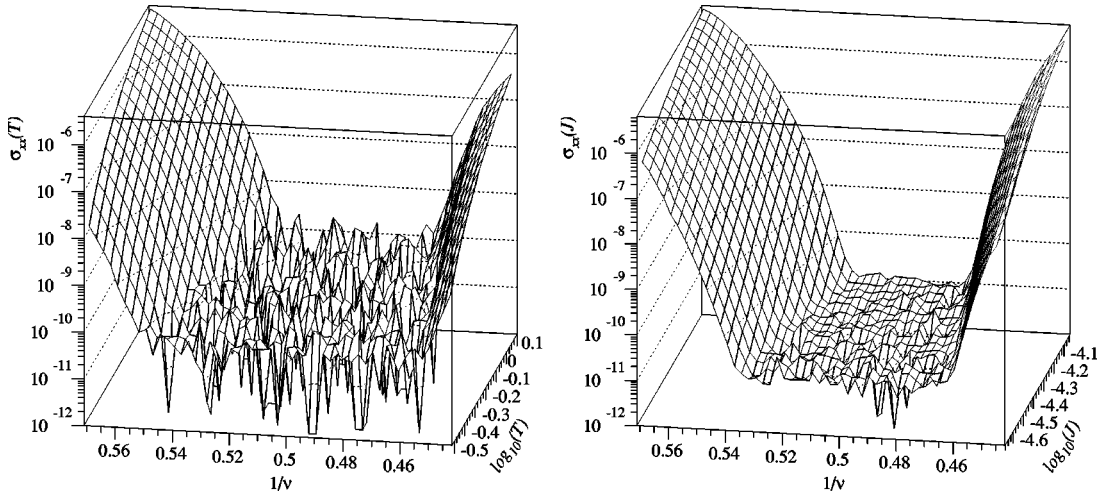
FIG. 6. Surface plots of the measured σ_{xx} on the second plateau as a function of temperature T (left) or current J (right). The ranges were chosen to show comparable σ_{xx}, and to correspond to the VRH regime. The saturation of σ_{xx} around the plateau center corresponds to experimental noise, which is decreasing in the $\sigma_{xx}(J)$ plot due to higher currents.

that range. On the high-ν side, however, the slope values typically differ by a factor of 4–6. The observed linear behavior of $\rho_{xy}(\rho_{xx})$ in both experiments (a) and (b) implies that the resistivities are dominated by the exponential term in Eqs. (2) and (6) for the dependence on T or J, respectively. Therefore, it must be the prefactors which differ in cases (a) and (b). One should keep in mind that the temperature-driven slopes represent thermally activated transport, whereas the current-driven results are obtained in the VRH regime. Therefore, we interpret the discrepancy in the slope values from the two experiments as a difference in the prefactors of the transverse resistivities due to different transport processes. Moreover, it was mentioned in Sec. III A that in the low-T range of VRH conduction, the deviations of $\delta\rho_{xy}(T)$ were much smaller than $\rho_{xx}(T)$, supporting the idea of transport-regime-dependent $\delta\rho_{xy}$ prefactors.

It is interesting to compare directly the conductivities obtained from both experiments (a) and (b). The σ_{xx} values measured on the second plateau as a function of temperature and current are shown in Fig. 6. The ranges of T and J were chosen to show comparable σ_{xx} values. Also, the T-range corresponds in this case to low temperatures with VRH conduction. The two plots are qualitatively very similar. We can now relate the quantities from both experiments by comparing the measured $\sigma_{xx}(T)\equiv\sigma_{xx}(J)$ point by point. This yields an effective electron temperature $T_{\text{eff}}=T[\sigma_{xx}(J)]$ for a given current J, as discussed in Sec. I. Results from this analysis for $T_{\text{eff}}(J)$ at three different ν are shown in Fig. 7. At low current levels, the measured conductivities are below the experimental noise, resulting in an artificially saturated T_{eff} ≈ 320 mK, which is simply the ^{3}He bath temperature. At higher J, however, a clear $T_{\text{eff}}(J)$ dependence is observed. Data analysis was performed in this way for all measured ν. The extracted effective temperatures were found to never exceed the range $T_{\text{eff}}=0.3,\ldots,1.4$ K. This justifies a treatment on the basis of hopping theory. If the temperature- and current-dependent conductivities obey the laws (4) and (6), respectively, we are able to relate the measurements according to

$$\left(\frac{\mathcal{E}_1}{\mathcal{E}_H}\right)^{\alpha_1}=\left(\frac{T_1}{T}\right)^{\alpha_2}+\ln\frac{\sigma_{xx}^{J}}{\sigma_{xx}^{T}}, \qquad (10)$$

with $\alpha_1,\alpha_2=\frac{1}{2}$ expected. To test this condition we applied a linear fit to the points at high J in the log-log plot (dotted lines in Fig. 7). The values of the slopes of the straight lines for all considered ν and for both samples are shown in the histogram (inset in Fig. 7). They correspond to the ratio α_1/α_2, and were found to be $\alpha_1/\alpha_2=1.005\pm0.096$. While $\alpha_2=\frac{1}{2}$ was already confirmed in Sec. III B, this result supports the interpretation of transport based on Eqs. (4) and (6). Finally, the position of the fitted straight lines yields the results for $T_1(\nu)/\mathcal{E}_1(\nu)$, which gives information on the localization length $\xi(\nu)$ [cf. Eq. (7)]. This is considered in Sec. IV.
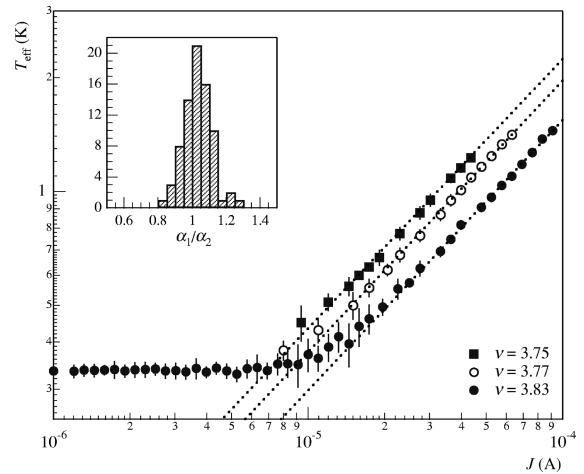

FIG. 7. Effective electron temperature T_{eff} vs current J in log-log representation, for three different filling factors. The data at low J, where T_{eff} saturates at about 0.32 K (which is the ^{3}He bath temperature), correspond to the range where σ_{xx} is in the experimental noise. The dotted lines are linear fits to the points at higher J. The inset shows the histogram of all slope values, with $\alpha_1/\alpha_2=1.005\pm0.096$.
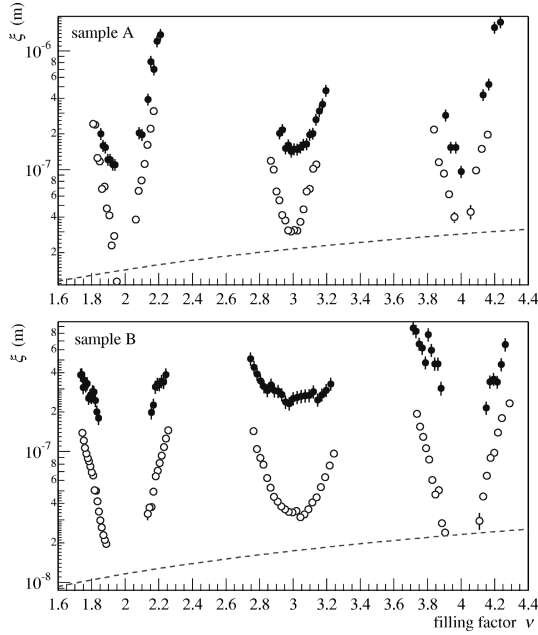
FIG. 8. Localization length ξ as a function of ν obtained from the two methods as discussed in the text. The open circles ○ are calculated from the characteristic hopping temperature T_1 (Fig. 5), and with Eq. (5). The full dots ● show the results from the effective electron temperature analysis (Sec. III C) of non-Ohmic transport data. The dashed lines correspond to the classical cyclotron radius R_c. The upper and lower figure are for samples A and B, respectively.

In the above argument we have neglected the additional term $\ln(\sigma_{xx}^J/\sigma_{xx}^T)$ in Eq. (10). It can, however, easily be seen from Fig. 5 that in most cases $\sqrt{T_1/T}$ is much larger than $\ln(\sigma_{xx}^J/\sigma_{xx}^T)$ even for possible differences of the prefactors by one order of magnitude (cf. the discussion above). If that were not true, no straight lines in $\ln(T_{\rm eff})$ versus $\ln(J)$ should have been observed, and slopes different from one should result. To be complete, this was indeed the case at certain ν values far away from the plateau center, where T_1 was very low. Such data were excluded from further analysis.

The same argument of negligible $\ln(\sigma_{xx}^J/\sigma_{xx}^T)$ also applies to the case where the behavior of the prefactors is not known exactly. Therefore, and this is most important, the experimental method and the way of data analysis discussed in this section allow us to investigate some fundamental relations in quantum transport even if certain parameters (like the functional behavior of the prefactors) are not perfectly determined.

IV. ANALYSIS AND DISCUSSION

In this section we will mainly focus on the results from the temperature- and current-dependent VRH conductivity measurements presented in Secs. III B and III C. Both experimental methods allow us to extract the localization length ξ. The values for $\xi(T_1)$ and $\xi[T_{\rm eff}(J)]$, calculated with Eqs. (5) and (7), respectively, are shown in Fig. 8. A constant dielectric function $\epsilon_r = 13$ was assumed in the case of $\xi(T_1)$. Close to the even-numbered plateau centers, no data points are available because of unmeasurably small re-

sistivities. The divergence of $\xi(\nu)$ for ν approaching half-filling fractions is well understood within the model of two-dimensional electron localization. Close to the LL center, the behavior of $\xi(\nu)$ is expected to follow the power law (1). For large energy separation $|E_c - E_F|$, i.e., E_F deep in the mobility gap between two LL's, the lack of knowledge about the exact form of the density of states does not allow us to deduce the functional behavior of the measured ξ explicitly. However, it is expected[6] that ξ approaches a length close to the classical cyclotron radius $R_c = \nu/\sqrt{2\pi n_e}$ for $\nu \rightarrow \nu_0$. This is indeed the case for $\xi(T_1)$. Compared to this prediction, the values of $\xi[T_{\rm eff}(J)]$ are anomalously large. The main formal difference between the two methods is that Eq. (5) includes the dielectric function ϵ_r (and the constant C), whereas Eq. (7) is based on the assumption of a homogeneous electric field. Different reasons may be found for the discrepancy between the localization lengths obtained from the two methods. The first criticism addresses the assumption of uniform electric field. Several theoretical[54] and experimental[55] investigations strongly suggest a significant charge and potential redistribution in the quantized regime. While the electrostatic potential in the metallic phase is essentially linear, the potential drops for filling factors close to integer mainly occur close to the sample edges, leading to strongly enhanced local field gradients. The width of these potential drops was observed to depend on external conditions like contacting geometry or an additional gate potential. In spite of theoretically predicted[56] narrow edge widths of less than 1 μm, there is also experimental evidence of a very wide region of up to 100 μm where the dominant potential drop occurs.[57] Concerning the electric-field-dependent hopping model (7), this picture leads to an effectively reduced sample width, being typically one order of magnitude smaller than the physical widths of our Hall bars. Taking such an estimate into account, the localization lengths $\xi[T_{\rm eff}(J)]$ should be reduced by the same amount towards R_c, and closely approach the values of $\xi(T_1)$ at the plateau centers.

Another reason for locally increased electric fields may be found in the macroscopically inhomogeneous nature of the samples.[58] Some spatially rare critical key resistances, composing the network of the infinite cluster where the current flows in the VRH regime, determine in first order the macroscopic resistance of the medium. While most of the potential drop occurs across such key resistances, the local field is enhanced there by the ratio of the characteristic distance of the critical sites and the hopping length. The latter is usually much smaller than the correlation radius of the infinite cluster. Although this effect may alter the effectively applied local electric fields, it is not clear how to quantify the model in our case. We realize, however, that both pictures of field inhomogeneity induced either at the sample edges or somewhere along the current path due to macroscopic impurities tend to account correctly for our experimental results. Our arguments are the following: although sample A has the higher electron mobility μ_e, it shows a significantly lower critical breakdown current J_c by about one order of magnitude compared to sample B (the latter having $J_c \simeq 600$ μA at $\nu = 2.0$). Hence, in spite of sample A's "higher electronic quality," it is less robust against increased $\mathcal{E}_H$. This is a consequence of a higher degree of macroscopic density fluctuation or large-scale impurities in sample A, governing the

transport properties under critical conditions, *in addition* to the smooth long-range random potential. The picture of the breakdown mechanism with large-scale distributed random impurities was recently investigated in Ref. 59. Those experiments confirmed the idea of a locally triggered breakdown at rare critical sites with enhanced electric field. The larger the number of macroscopic impurities (or the larger the sample), the higher the probability to exceed the critical threshold at such a site. Taking this into account in the context of the discussed locally increased field within the VRH model, one would expect a better agreement between $\mathcal{E}_H$ and the average effective local field for sample A. This is indeed consistent with our $\xi[T_{\text{eff}}(J)]$ results, which show lower values for sample A, being in better agreement with predictions and the temperature-dependent VRH experiment. On the other hand, sample A is half as wide as sample B, i.e., the physical width is closer to the potential drop width in the scenario of increased field at the sample edges. This again leads to lower $\xi[T_{\text{eff}}(J)]$ for sample A, as observed in the data. To conclude this discussion, more experiments are needed to distinguish the field enhancement mechanisms and to answer the question about the dominant contribution.

Next, we want to comment on the $\xi(T_1)$ values related to the temperature-dependent experiment. Although the dielectric function ϵ_r appearing in Eq. (5) is usually assumed to be constant in the two-dimensional case, this is a crude approximation, and is neither theoretically nor experimentally established. In real systems, the dielectric function is believed to diverge in the three-dimensional case when approaching the LL center.[60] Drawing the analogy for the quantum Hall effect in two dimensions, the dielectric function grows like $\epsilon_r \propto \xi^\beta$ with $0 \leq \beta \leq 1$.[30] Since our experiment in the VRH temperature regime actually measures $\epsilon_r \xi(T_1)$ as a function of ν according to Eq. (5), the ratio between our $\xi(T_1)$ (where a constant $\epsilon_r = 13$ was assumed above) and $\xi[T_{\text{eff}}(J)]$ gives the relative behavior of $\epsilon_r(\nu)$, under the assumption that everything else varies at a negligible level relative to $\xi(\nu)$. As far as the local electric-field distribution or the field enhancement mechanisms is concerned, the latter condition of invariance is not necessarily true. We will, however, shortly give an intuitive argument justifying our approach. The dielectric function

$$\epsilon_r(\nu) = \frac{Ce^3 \mathcal{E}_1}{8\pi\epsilon_0 k_B^2 T_1^2}, \qquad (11)$$

deduced from the experimental data and based on Eqs. (5) and (7), is plotted in Fig. 9. The reduced ϵ_r around integer ν compared to the GaAs bare value is due to the underestimate of the electric field by about one order of magnitude, as discussed above. The systematic divergence of $\epsilon_r(\nu)$ with decreasing $|E_F - E_c|$ is clearly observed here for two-dimensional electron systems in the quantum Hall regime. For sample B, the significant effect appears symmetric with respect to integer ν_0, whereas the weak asymmetry observed for sample A is attributed to a slight shift of the electron densities between the two experiments. A fit of the assumed power-law dependence to the points ϵ_r versus $\xi[T_{\text{eff}}(J)]$ for all ν yields the exponent $\beta = 1.098 \pm 0.096$, independent of LL index. This result is in agreement with theoretical con-
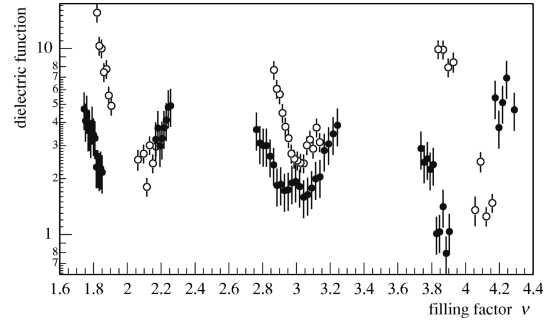

FIG. 9. Dielectric function, given by the ratio $\epsilon_r \propto \xi(T_1)/\xi(T_{\text{eff}})$, vs filling factor ν. Open circles $\bigcirc$ and full dots $\bullet$ represent the results for samples A and B, respectively. The divergence of the ratio with decreasing distance between Fermi level and the LL center implicitly suggests a divergence of the dielectric function $\epsilon_r(\nu)$.

siderations about a filling-factor-dependent dielectric function, although it has not been experimentally observed before.

We argued above that the functional behavior of the experimentally determined $\epsilon_r(\nu)$ reflects the divergent dielectric function and not a variation of $\xi(T_{\text{eff}})$ due to ν-dependent electric-field distribution effects. The reason why we conclude this, is the following: the distance $|E_F - E_c|$ in the spin gap (third plateau) is small enough (in contrast to plateaus 2 and 4) to potentially observe the power-law divergence of the localization length according to Eq. (1). There the critical exponent γ was found [from fitting Eq. (1) to the $\xi(\nu)$ data points] to be $\gamma = 2.29 \pm 0.21$ in the case of $\xi[T_{\text{eff}}(J)]$ and $\gamma = 4.61 \pm 0.24$ for $\xi(T_1)$. Hence the critical exponent in the former case is very consistent with the theoretically predicted value ~ 2.3, whereas in the latter case γ is too large by a factor of 2 [we should mention, that we are not in the situation here of two strongly overlapping spin levels, which might lead to an enhanced critical exponent by a factor of 2 (Ref. 30)]. This result justifies the assumption made above of a negligible effective electric-field variation within our ν range. It rather supports the picture where $\xi(T_1)$ in Fig. 8 actually represents the measurement of $\epsilon_r(\nu)\xi(\nu)$, with $\epsilon_r \propto \xi$. Although this argument is consequently based on our experimental results, more measurements on extended ν and temperature ranges are needed to investigate the subject (possibly with other high-mobility samples), and to confirm its implications on the electrical properties in the quantized Hall regime.

V. CONCLUSIONS

Results from a large series of transport measurements on quantum Hall bars have been reported. We clearly distinguish between thermally activated transport and transport dominated by VRH. In the former case, the longitudinal conductance in our high-mobility samples agreed well with the Arrhenius Law. The extrapolated prefactors were found to be $(2.02 \pm 0.11)e^2/h$ within a narrow range around the plateau centers. Deviations $\delta\rho_{xy}$ of the transverse resistivity from the quantized value were attributed to a mixing of ρ_{xx} into ρ_{xy} due to finite probe arm widths on one hand, and to thermal activation $\delta\rho_{xy} \propto e^{-T_0/T}$ with the activation energy T_0 on the

other hand. The activation energy T_0 was shown to be the same for both $\rho_{xx}(T)$ and $\delta\rho_{xy}(T)$. The observed strong asymmetry of $\delta\rho_{xy}/\rho_{xx}$ with respect to the plateau center was explained with an asymmetry of the ρ_{xx} prefactors due to either percolating full or percolating empty transport regimes.

At lower temperatures, both temperature and current dependent longitudinal conductivity could be well understood on the basis of a VRH theory[15,20] taking a Coulomb gap into account. Those experiments allowed to determine the localization length $\xi(\nu)$ in two different ways. The divergence of ξ for E_F approaching the LL center could be demonstrated in the quantum Hall effect over a relatively broad ν range. An inhomogeneous electric-field distribution (either due to edge effects or macroscopic impurities) was considered to explain discrepancies between the two methods. Most interestingly, our experimental results suggest a divergence of the dielectric function ϵ_r. First, this divergence was deduced from the ratio $\xi(T_1)/\xi(T_{\text{eff}})$ of the two differently obtained sets of ξ values, according to Eq. (11): $\xi(T_1)$ contains ϵ_r, and the ratio diverges on the third plateau like $|\nu-\nu_c|^{-2.3}$ (see Fig. 9). Second, the critical localization exponent was found to be equal to the theoretical value $\gamma\simeq2.3$ for the ϵ_r-independent model, or twice that value in the case of the ϵ_r-dependent model. Hence, the experiment in the latter case measured $\epsilon_r\xi$ with $\epsilon_r\propto\xi$. We suggest further measurements, with the experimental range extended to larger ν and lower temperatures, in order to verify our conclusions and to determine the ξ values at the resistivity minima as a function of ν.

[1] For a review, see *The Quantum Hall Effect*, edited by R. E. Prange and S. M. Girvin (Springer-Verlag, Berlin, 1990).

[2] H. P. Wei, D. C. Tsui, M. A. Paalanen, and A. M. M. Pruisken, Phys. Rev. Lett. **61**, 1294 (1988).

[3] A. M. M. Pruisken, Phys. Rev. Lett. **61**, 1297 (1988).

[4] G. V. Mil'nikov and I. M. Sokolov, Pis'ma Zh. Éksp. Teor. Fiz. **48**, 494 (1988) [JETP Lett. **48**, 536 (1988)]; J. T. Chalker and P. D. Coddington, J. Phys. C **21**, 2665 (1988); Y. Hou and R. N. Bhatt, Phys. Rev. Lett. **68**, 1375 (1992).

[5] S. Koch, R. J. Haug, K. von Klitzing, and K. Ploog, Surf. Sci. **263**, 108 (1992).

[6] M. M. Fogler, A. Yu. Dobin, and B. I. Shklovskii, Phys. Rev. B **57**, 4614 (1998).

[7] D.-H. Lee, S. Kivelson, and S.-C. Zhang, Phys. Rev. Lett. **68**, 2386 (1992); **71**, 2679 (1993); R. N. Bhatt, N. Read, and B. Huckestein, *ibid.* **71**, 2678 (1993); S. Das Sarma and D. Liu, Phys. Rev. B **48**, 9166 (1993); S. S. Mandal and V. Ravishankar, *ibid.* **55**, 15 748 (1997).

[8] D. G. Polyakov and B. I. Shklovskii, Phys. Rev. Lett. **73**, 1150 (1994).

[9] D. G. Polyakov and B. I. Shklovskii, Phys. Rev. Lett. **74**, 150 (1995).

[10] M. M. Fogler and B. I. Shklovskii, Solid State Commun. **94**, 503 (1995); M. M. Fogler, D. G. Polyakov, and B. I. Shklovskii, Surf. Sci. **361/362**, 255 (1996).

[11] K. Yoshihiro, J. Kinoshita, K. Inagaki, C. Yamanouchi, J. Moriyama, and S. Kawaji, Physica B & C **117B**, 706 (1983): M. E. Cage, B. F. Field, R. F. Dziuba, S. M. Girvin, A. C. Gossard, and D. C. Tsui, Phys. Rev. B **30**, 2286 (1984).

[12] H. P. Wei, D. C. Tsui, and A. M. M. Pruisken, Phys. Rev. B **33**, 1488 (1985).

[13] I. Ruzin and S. Feng, Phys. Rev. B **74**, 154 (1995).

[14] H. P. Wei, L. W. Engel, and D. C. Tsui, Phys. Rev. B **50**, 14 609 (1994); E. Chow and H. P. Wei, *ibid.* **52**, 13 749 (1995); H. Scherer, L. Schweitzer, F. J. Ahlers, L. Bliek, R. Lösch, and W. Schlapp, Semicond. Sci. Technol. **10**, 959 (1995).

[15] B. I. Shklovskii and A. L. Efros, *Electronic Properties of Doped Semiconductors* (Springer, Berlin, 1984).

[16] G. Ebert, K. von Klitzing, C. Probst, E. Schuberth, K. Ploog, and G. Weimann, Solid State Commun. **45**, 625 (1983).

[17] A. Briggs, Y. Guldner, J. P. Vieren, M. Voos, J. P. Hirtz, and M. Razeghi, Phys. Rev. B **27**, 6549 (1983).

[18] N. F. Mott, J. Non-Cryst. Solids **1**, 1 (1968); N. F. Mott and E. A. Davis, *Electronic Processes in Non-Crystalline Materials*, 2nd ed. (Clarendon, Oxford, 1979).

[19] M. Pollak, Discuss. Faraday Soc. **50**, 13 (1970).

[20] A. L. Efros and B. I. Shklovskii, J. Phys. C **8**, L49 (1975).

[21] V. L. Nguyen, Fiz. Tekh. Poluprovodn. **18**, 335 (1984) [Sov. Phys. Semicond. **18**, 207 (1984)].

[22] Y. Ono, J. Phys. Soc. Jpn. **51**, 237 (1982).

[23] K. I. Wysokinski and W. Brenig, Z. Phys. B **54**, 11 (1983).

[24] A. Grunwald and J. Hajdu, Z. Phys. B **78**, 17 (1990).

[25] S. Koch, R. J. Haug, K. von Klitzing, and K. Ploog, Semicond. Sci. Technol. **10**, 209 (1995).

[26] F. W. Van Keuls, X. L. Hu, H. W. Jiang, and A. J. Dahm, Phys. Rev. B **56**, 1161 (1997).

[27] P. Středa and K. von Klitzing, J. Phys. C **17**, L483 (1984); L. Eaves and F. J. Sheard, Semicond. Sci. Technol. **1**, 346 (1986); V. L. Pokrovsky, L. P. Pryadko, and A. L. Talpov, J. Phys. C **2**, 1583 (1990); P. Bøggild and E. B. Hansen, Phys. Scr. **T69**, 124 (1997).

[28] S. A. Trugman, Phys. Rev. B **27**, 7539 (1983).

[29] P. W. Anderson, E. Abrahams, and T. V. Ramakrishnan, Phys. Rev. Lett. **43**, 718 (1979); G. Ebert, K. von Klitzing, K. Ploog, and G. Weimann, J. Phys. C **16**, 5441 (1983); S. Komiyama, T. Takamasu, S. Hiyamizu, and S. Sasa, Solid State Commun. **54**, 479 (1985).

[30] D. G. Polyakov and B. I. Shklovskii, Phys. Rev. B **48**, 11 167 (1993).

[31] B. I. Shklovskii, Fiz. Tekh. Poluprovodn. **6**, 2335 (1972) [Sov. Phys. Semicond. **6**, 1964 (1973)]; B. I. Shklovskii, E. I. Levin, H. Fritzsche, and S. D. Baranovskii, in *Transport, Correlation and Structural Defects*, edited by H. Fritzsche (World Scientific, Singapore, 1990).

[32] B. J. van Wees, E. M. M. Willems, L. P. Kouwenhoven, C. J. P. M. Harmans, J. G. Williamson, C. T. Foxon, and J. J. Harris, Phys. Rev. B **39**, 8066 (1989); S. Komiyama and H. Nii, Physica B **184**, 7 (1993): C. A. Richter, R. G. Wheeler, and R. N. Sacks, Surf. Sci. **305**, 145 (1994).

[33] P. A. Crump, B. L. Gallagher, T. Cheng, J. Middleton, and A. Jezierski, Semicond. Sci. Technol. **9**, 1455 (1994).

[34] B. Jeckelmann, B. Jeanneret, and D. Inglis, Phys. Rev. B **55**, 13 124 (1997); B. Jeckelmann and B. Jeanneret, IEEE Trans. Instrum. Meas. **46**, 276 (1997).

[35] S. Komiyama and H. Hirai, Phys. Rev. B **40**, 7767 (1989); H. Hirai and S. Komiyama, J. Appl. Phys. **68**, 655 (1990).

[36] R. J. Haug, Semicond. Sci. Technol. **8**, 131 (1993).

[37] N. B. Zhitenev, R. J. Haug, K. v. Klitzing, and K. Eberl, Phys. Rev. B **51**, 17 820 (1995); T. Machida, H. Hirai, S. Komiyama, T. Osada, and Y. Shiraki, *ibid.* **54**, R14261 (1996).

[38] R. J. Haug, K. von Klitzing, and K. Ploog, Phys. Rev. B **35**, 5933 (1987); R. J. Haug, R. R. Gerhardts, K. von Klitzing, and K. Ploog, Phys. Rev. Lett. **59**, 1349 (1987).

[39] P. Svoboda, P. Středa, G. Nachtwei, A. Jaeger, M. Cukr, and M. Láznička, Phys. Rev. B **45**, 8763 (1992).

[40] G. Nachtwei, S. Heide, C. Breitlow, P. Svoboda, and M. Cukr, Phys. Rev. B **50**, 8488 (1994); G. Nachtwei, C. Breitlow, J. Seyfarth, S. Heide, L. Bliek, F.-J. Ahlers, P. Svoboda, and M. Cukr, Semicond. Sci. Technol. **9**, 10 (1994).

[41] M. Furlan, Physica B (Amsterdam) **249-251**, 123 (1998).

[42] T. Ando and Y. Uemura, J. Phys. Soc. Jpn. **37**, 1044 (1974).

[43] Th. Englert, D. C. Tsui, A. C. Gossard, and Ch. Uihlein, Surf. Sci. **113**, 295 (1982); R. J. Nicholas, R. J. Haug, K. von Klitzing, and G. Weimann, Phys. Rev. B **37**, 1294 (1988); A. Usher, R. J. Nicholas, J. J. Harris, and C. T. Foxon, *ibid.* **41**, 1129 (1990).

[44] V. T. Dolgopolov, A. A. Shashkin, A. V. Aristov, D. Schmerek, W. Hansen, J. P. Kotthaus, and M. Holland, Phys. Rev. Lett. **79**, 729 (1997).

[45] P. Svoboda, G. Nachtwei, C. Breitlow, S. Heide, and M. Cukr, Semicond. Sci. Technol. **12**, 264 (1997).

[46] R. G. Clark, J. M. Mallett, S. R. Haynes, J. J. Harris, and C. T. Foxon, Phys. Rev. Lett. **60**, 1747 (1988); R. G. Clark, Phys. Scr. **T39**, 45 (1991); Y. Katayama, D. C. Tsui, and M. Shayegan, Phys. Rev. B **49**, 7400 (1994); S. I. Dorozhkin, M. O. Dorokhava, R. J. Haug, K. von Klitzing, and K. Ploog, Pis'ma Zh. Éksp. Teor. Fiz. **63**, 67 (1996) [JETP Lett. **63**, 76 (1996)].

[47] W. van der Wel, C. J. P. M. Harmans, J. E. Mooij, J. Phys. C **21**, L171 (1988).

[48] For a review, see B. Huckestein, Rev. Mod. Phys. **67**, 357 (1995).

[49] N. R. Cooper and J. T. Chalker, Phys. Rev. B **48**, 4530 (1993).

[50] Q. Du, H. Xu, P. Ramvall, and P. Omling, Phys. Rev. B **55**, R7355 (1997); J. Oswald, G. Span, and F. Kuchar, cond-mat/9707105.

[51] B. W. Alphenaar, P. L. McEuen, R. G. Wheeler, and R. N. Sacks, Physica B **175**, 235 (1991); S. Komiyama, H. Hirai, M. Ohsawa, Y. Matsuda, S. Sasa, and T. Fujii, Phys. Rev. B **45**, 11 085 (1992).

[52] D. Weiss, K. von Klitzing, and V. Mosser, in *Two-Dimensional Systems: Physics and New Devices*, edited by G. Bauer, F. Kuchar, and H. Heinrich, Springer Series in Solid State Physics Vol. 67 (Springer, Berlin, 1986), p. 204.

[53] B. I. Shklovskii, Pis'ma Zh. Éksp. Teor. Fiz. **36**, 43 (1982) [JETP Lett. **36**, 51 (1982)].

[54] P. K. Yogeshwar and W. Brenig, Europhys. Lett. **7**, 737 (1988); D. Pfannkuche and J. Hajdu, Phys. Rev. B **46**, 7032 (1992); D. J. Thouless, Phys. Rev. Lett. **71**, 1879 (1993); A. Shik, J. Phys. C **5**, 8963 (1993); C. Wexler and D. J. Thouless, Phys. Rev. B **49**, 4815 (1994); M. E. Cage and C. F. Lavine, J. Res. Natl. Inst. Stand. Technol. **100**, 529 (1995).

[55] H. Z. Zheng, D. C. Tsui, and A. M. Chang, Phys. Rev. B **32**, 5506 (1985); E. K. Sichel, H. H. Sample, and J. P. Salerno, *ibid.* **32**, 6975 (1985); G. Ebert, K. von Klitzing, and G. Weimann, J. Phys. C **18**, L257 (1985); Ch. Simon, B. B. Goldberg, F. F. Fang, M. K. Thomas, and S. Wright, Phys. Rev. B **33**, 1190 (1986).

[56] D. B. Chklovskii, B. I. Shklovskii, and L. I. Glazman, Phys. Rev. B **46**, 4026 (1992).

[57] P. F. Fontein, P. Hendriks, F. A. P. Blom, J. H. Wolter, L. J. Giling, and C. W. J. Beenakker, Surf. Sci. **263**, 91 (1992); D. J. McKitterick, A. Shik, A. J. Kent, and M. Henini, Phys. Rev. B **49**, 2585 (1994); A. A. Shashkin, A. J. Kent, P. Harrison, K. R. Strickland, L. Eaves, and M. Henini, Semicond. Sci. Technol. **9**, 2110 (1994); S. Takaoka, K. Oto, K. Kurimoto, K. Murase, K. Gamo, and S. Nishi, Phys. Rev. Lett. **72**, 3080 (1994); R. J. F. van Haren, F. A. P. Blom, and J. H. Wolter, *ibid.* **74**, 1198 (1995); W. Dietsche, K. von Klitzing, and K. Ploog, Surf. Sci. **361/362**, 289 (1996).

[58] I. G. Austin and M. Sayer, J. Phys. C **7**, 905 (1974); B. I. Shklovskii, Fiz. Tekh. Poluprovodn. **10**, 1440 (1976) [Sov. Phys. Semicond. **10**, 855 (1976)]; O. Faran and Z. Ovadyahu, Solid State Commun. **67**, 823 (1988).

[59] G. Nachtwei, G. Lütjering, D. Weiss, Z. H. Liu, K. von Klitzing, and C. T. Foxon, Phys. Rev. B **55**, 6731 (1997); V. Tsemekhman, K. Tsemekhman, C. Wexler, J. H. Han, and D. J. Thouless, *ibid.* **55**, R10201 (1997).

[60] T. G. Caster, N. K. Lee, G. S. Cieloszyk, and G. L. Salinger, Phys. Rev. Lett. **34**, 1627 (1975); V. E. Dubrov, M. E. Levinshtein, and M. S. Shur, Zh. Éksp. Teor. Fiz. **70**, 2014 (1976) [Sov. Phys. JETP **43**, 1050 (1976)]; A. L. Efros and B. I. Shklovskii, Phys. Status Solidi B **76**, 475 (1976): W. L. McMillan, Phys. Rev. B **24**, 2739 (1981): H. F. Hess, K. DeConde, T. F. Rosenbaum, and G. A. Thomas, *ibid.* **25**, 5578 (1982); Y. Imry, Y. Gefen, and D. J. Bergman, *ibid.* **26**, 3436 (1982).